

Scatter and Attenuation Correction in Technetium-99m Brain SPECT

Jun Hashimoto, Atsushi Kubo, Koichi Ogawa, Takahiro Amano, Yasuo Fukuuchi, Nobutoku Motomura and Takashi Ichihara
Department of Radiology, Department of Internal Medicine, School of Medicine, Keio University, Shinjuku-ku, Tokyo;
Department of Electronic Informatics, College of Engineering, Hosei University, Koganei-shi, Tokyo; Toshiba Medical
Engineering Laboratory, Shimoishigami, Ohtawara-shi, Tochigi, Japan

We propose a practical method for scatter and attenuation compensation in ^{99m}Tc -ECD brain SPECT using a simultaneous emission CT (ECT) and transmission CT (TCT) acquisition system that includes the following major components: (a) triple-headed SPECT gamma camera equipped with fanbeam collimators; (b) external line sources containing ^{99m}Tc placed at the focal lines of the collimators; and (c) scatter correction by the triple-energy-window (TEW) method. **Methods:** Projection images were obtained over a 360° rotation scan. After acquisition, scatter correction was performed using the TEW method, which corrected scattered photons pixel by pixel in the projection data. Scatter-corrected ECT images were compensated for attenuation using the TCT images with Chang's iterative method, and were converted to activity concentration (kBq/ml) images by obtaining a cross-calibration scan. After validating this method with phantom studies, it was applied to clinical brain imaging using a combination of 925 MBq ^{99m}Tc -ECD as a radiopharmaceutical and 222 MBq ^{99m}Tc as an external source. ECT and TCT data were acquired separately or simultaneously. **Results:** SPECT quantification and image quality were improved by performing this correction. The activity concentration images obtained with the simultaneous acquisition were almost identical to those obtained with the separate acquisition. **Conclusion:** This method was clinically practical and cost-effective for reconstructing quantitative ^{99m}Tc brain SPECT images.

Key Words: brain SPECT; transmission CT; attenuation correction; triple-energy window scatter correction; technetium-99m-ECD

J Nucl Med 1997; 38:157-162

The presence of photon attenuation and scattering limits the accuracy of quantification of tracer activity in radionuclide imaging with a gamma camera system. Some of the scattered photons are measured as having almost the same energy as the primary photons, so these photons are detected as primary photons in the photopeak energy window. According to some reports using Monte Carlo methods, the amount of scattered photons in a projection image varies depending on the distribution of the scatterer and the distribution of the radioactive source (1,2). It is therefore necessary to estimate scattered photons for each pixel in projection data. To approach the problem, we proposed a triple-energy window (TEW) scatter-correction method that corrects scattered photons for each pixel (3-5).

Attenuation correction used to be performed assuming uniform distribution of attenuation coefficients (6-9). Recently, for more accurate correction, new methods have been reported that consider nonuniform distribution of attenuation coefficients (10-21). Some investigators used transmission CT (TCT) techniques to obtain attenuation coefficient maps (10,11,13-17,21). We present a practical technique for clinical studies that

uses the TEW method for scatter compensation and TCT images for attenuation correction.

MATERIALS AND METHODS

Data Acquisition

All images in this study were acquired with a three-headed rotating camera, dedicated SPECT system equipped with fanbeam collimators. Focal lines of the collimators are located at the apexes of the triangle made by three detectors as shown in Figure 1. We performed two kinds of data acquisition protocols: a sequential mode and a simultaneous mode.

Sequential Mode. In the sequential mode, two separate scans are required for transmission and emission data acquisition. The sequential mode includes two subtypes: the T3-I-E3 and I-T3-E3 methods, in which T3 means transmission scan using three detectors; I means injection; and E3 means emission scan using three detectors. In the T3-I-E3 method, a transmission scan was obtained using three detectors before tracer administration. We placed a ^{99m}Tc line source at the focal line of each collimator. Each line source contained about 222 MBq ^{99m}Tc . The transmission scan used a 120° continuous rotation of each detector and a total scan time of 15 min. A 20% energy window centered at the 140-keV photopeak and a 128×128 matrix were used for data acquisition. An attenuation coefficient map was obtained by reconstructing the transmission data into a 128×128 matrix using a filtered backprojection method with the Shepp-Logan filter. This transmission scan does not require any scatter compensation because the geometry of the fanbeam collimators reject almost all of the scattered photons from the transmission sources (22). After the transmission scan, 925 MBq ^{99m}Tc -ECD were injected without moving the patient. Then, an emission scan with 120° continuous rotation for a total scan time of 15 min was also obtained.

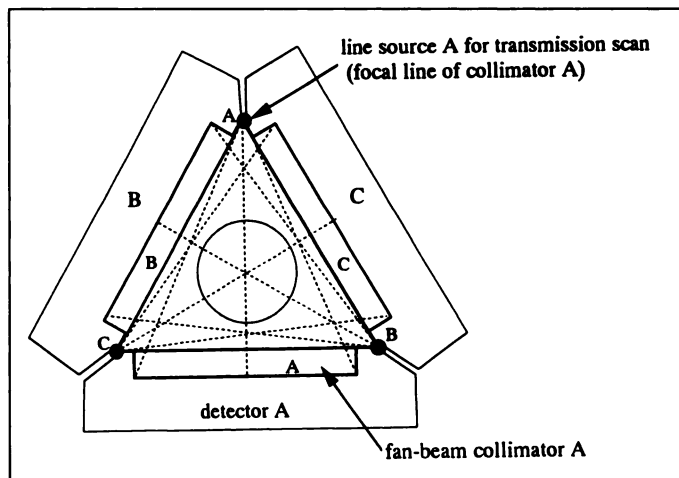


FIGURE 1. Geometric configurations of detectors, collimators and transmission sources.

Received Aug. 21, 1995; revision accepted Apr. 4, 1996.

For correspondence or reprints contact: Jun Hashimoto MD, Department of Radiology, School of Medicine, Keio University, 35 Shinanomachi, Shinjuku-ku, Tokyo, 160 Japan.

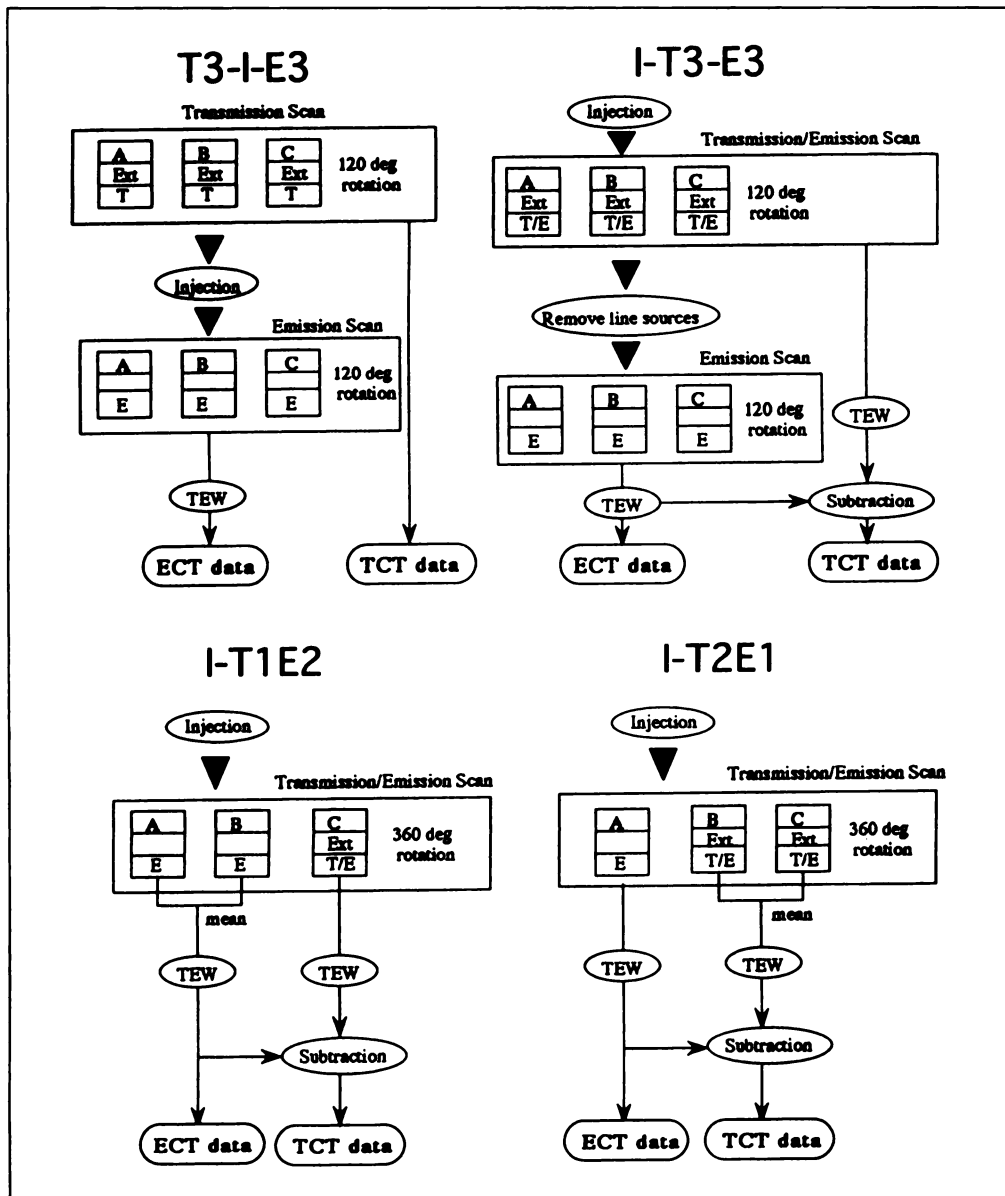


FIGURE 2. Four imaging protocols: A-C = detector; Ext = external source (^{99m}Tc); T = transmission raw data; E = emission raw data; T/E = transmission data including emission data; and TEW = triple-energy window scatter correction.

Projection images were acquired using a width of 20% (28 keV) for the main window centered at the 140-keV photopeak and a width of 7% (10 keV) for the lower subwindow centered at 121 keV. A Butterworth filter with a 0.44 cutoff frequency (cycles/cm) was applied to the projection images acquired using the main window and a 0.21 cutoff frequency was applied to the other projection images measured using the subwindow (4). Both of the filters were order 8. Primary counts in the projection data were calculated by the TEW method. After the TEW scatter correction, fanbeam to parallel-beam transformation; and intrinsic and extrinsic sensitivity correction were performed. Filtered backprojection images were reconstructed into a 128×128 matrix with the Shepp-Logan filter.

In the I-T3-E3 method, emission and transmission scans were performed simultaneously. Then a second emission scan was obtained after removing the three line sources. After the TEW scatter correction, the count data of the emission scan were subtracted from those of the simultaneous scan to obtain the pure transmission data. This subtraction was done at each sampling angle using sets of projection data at the same sampling position. Pure emission images were corrected for physical decay to the time of the simultaneous scan before the subtraction. Image processing

and reconstruction methods were the same as those in the T3-I-E3 method.

Simultaneous Mode. Simultaneous mode requires only a single 360° rotation scan. This mode also is divided into two subtypes: the I-T1E2 and I-T2E1 methods. In the I-T1E2 method, a transmission source was placed at the focal line of only one of the three collimators. By performing a simultaneous transmission-emission scan, one detector collects transmission-emission combined data and two detectors collect only emission data. The geometry of the fanbeam collimators rejects photons that were emitted from the external source and scattered in the patient (22). Both of fanbeam collimators and the TEW method reject scattered photons emitted from the tracer. Transmission data were obtained by subtracting the mean of the emission data acquired by two detectors at a given angle from the transmission-emission data acquired by one detector at the same angle. The image processing and reconstruction methods are the same methods used in the sequential mode. In the I-T2E1 method, transmission sources were placed at the focal lines of two collimators. During the simultaneous scan, two detectors acquire transmission-emission data and one detector acquires emission data. Figure 2 summarizes the four acquisition protocols mentioned above.

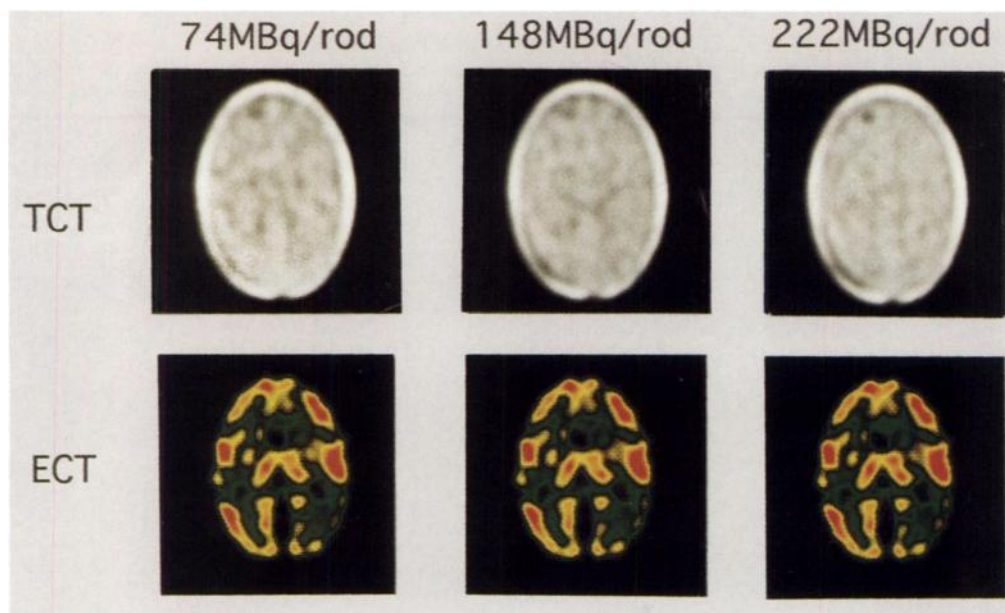


FIGURE 3. Effect of external source activities on TCT and ECT images. ECT images are displayed with an absolute scale.

Compensation

TEW Methods for Scatter Compensation. The TEW method requires three windows for data acquisition: a main window centered at the photopeak and two subwindows on both sides of the main window (3,4). In clinical studies using ^{99m}Tc , we used a combination of a 20% main window and a 7% subwindow (5). The lower subwindow was enlarged to improve S/N ratio and the upper subwindow was not used to avoid statistical noise due to lower counts. Based on the Monte Carlo simulation, it has been shown that a two-window image acquisition is sufficient for ^{99m}Tc (1,3,5). With the main window; we acquire the total count (Ctotal) that is composed of the count of primary photons (Cprim) and that of scattered photons. Cprim is estimated by the following equation:

$$C_{\text{prim}} = C_{\text{total}} - C_{\text{low}}/W_{\text{s}} \times W_{\text{m}}/2,$$

where C_{low} is the count in the lower subwindow and W_{s} and W_{m} are the widths of the the lower subwindow and the main window, respectively. Thus, the TEW method actually turned into a two-energy-window technique in this study using ^{99m}Tc -ECD and ^{99m}Tc external sources.

Modified Correction Matrix Methods for Attenuation Correction. For attenuation correction, we used a modified correction matrix (MCM) method (10), which is a modified version of Chang's iterative method (6). The method uses a measured attenuation coefficient map which is the two-dimensional distribution of linear attenuation coefficients obtained by gamma ray transmission CT. Attenuation correction is performed by multiplying scatter-corrected ECT data (reconstructed data) by a correction matrix. In other words, we used a matrix containing the correction coefficient for each pixel obtained from the attenuation map. The correction coefficient is the reciprocal of the mean of the attenuation ratio in all directions of projection from each position (pixel). Three iterations were performed.

Phantom Studies

Measurement of Absorbed Dose. Absorbed dose was measured by thermoluminescent dosimetry (TLD) during a 15-min transmission scan obtained with three rods of 370 MBq ^{99m}Tc . Six dosimeters (BeO, 1 mm ϕ \times 10 mm, cylindrical) were laid out on the surface of the brain phantom and we performed two transmission scans. In the TLD, calibration was performed in an acrylic phantom using 37 GBq of ^{137}Cs as a calibration source.

Determination of Appropriate External Source Activity. In all of the following phantom studies, the brain phantom (185 \times 130 mm, elliptical) was wrapped with a layer of plaster-barium mixture to simulate the skull bone (6 mm thick). We used the same choices of acquisition and processing parameters with conventional methods and our method. Square ROIs with 4 \times 4 pixels were used to obtain count data. A cross-calibration scan was obtained to quantify the actual value of activity concentration as follows. Technetium-99m (0.3 ml) was placed in a syringe approximately 5.0 mm in diameter and suspended in the air during scanning to minimize the effect of photon scattering and attenuation. Then, a single-thick slice, a transaxial SPECT image covering the entire activity was reconstructed and a large ROI was set surrounding the entire area. The cross-calibration factor was obtained between the counts in the ROI and those measured by a Curie meter for evaluation.

Technetium-99m activities of 74 MBq, 148 MBq and 222 MBq rods were evaluated to find the appropriate activity of the external line source. A brain phantom was prepared by simulating an injection of 925 MBq ^{99m}Tc -ECD. The cortex and thalamus compartments of the phantom were filled with ^{99m}Tc (50.0 kBq/ml) and the white-matter compartments with 20.6 kBq/ml. The T3-I-E3 method was used for data acquisition.

Separation of Transmission and Emission Data. A phantom study was obtained to elucidate the accuracy of separation of transmission data and emission data. The gray-matter compart-

TABLE 1
External Source Activity and Accuracy of SPECT Quantification

External source activity	74 MBq	148 MBq	222 MBq	True value
Attenuation coefficients for water (cm^{-1})	0.145 \pm 0.007	0.150 \pm 0.006	0.150 \pm 0.005	0.154
Cross-calibrated SPECT values (kBq/ml)				
Cortex	47.4 \pm 1.9	49.2 \pm 2.2	49.2 \pm 1.1	50.0
White matter	22.2 \pm 0.4	21.5 \pm 0.4	21.5 \pm 0.4	20.6

TABLE 2
Attenuation Coefficients and Cross-Calibrated SPECT Values in Simultaneous Acquisitions

	I-T3-E3	I-T1-E2	TCT only	True value
Attenuation coefficients (liter/cm)				
For water	0.148 ± 0.005	0.146 ± 0.007	0.147 ± 0.005	0.154
For skull-simulating wrap	0.228 ± 0.013	0.217 ± 0.012	0.203 ± 0.010	—
Cross-calibrated SPECT values (kBq/ml)				
Cortex				
SC + AC	42.9 ± 1.1	42.9 ± 0.7	—	43.3
w/o C	20.5 ± 0.4	20.1 ± 0.3	—	—
SC only	16.2 ± 0.3	16.0 ± 0.3	—	—
AC only	54.1 ± 1.3	53.7 ± 1.0	—	—
White matter				
SC + AC	17.4 ± 0.4	16.7 ± 0.4	—	18.1
w/o C	10.6 ± 0.3	9.3 ± 0.3	—	—
SC only	5.7 ± 0.3	5.1 ± 0.3	—	—
AC only	30.2 ± 0.7	26.7 ± 0.7	—	—

SC = scatter correction; AC = attenuation correction; w/o C = without correction.

ments of the phantom were filled with 43.3 kBq/ml and the white-matter compartments with 18.1 kBq/ml. The I-T3-E3 and I-T1E2 methods were used for acquisition. Scatter and attenuation corrected images obtained with the I-T1E2 method were compared with those of the I-T3-E3 method. We also performed TCT of the phantom without emission pharmaceuticals.

Clinical Evaluation. Two normal volunteers were enrolled in clinical studies using 925 MBq ^{99m}Tc-ECD. One volunteer was referred only for the T3-I-E3 protocol. The other was referred for all four acquisition protocols. Scans were started 15 min after the administration. We made count profile curves from images with and without correction.

RESULTS

In thermoluminescent dosimetry, data at the 12 measuring points were obtained. Mean absorbed dose was 0.22 ± 0.02 mSv. The maximum value and the minimum value was 0.25 mSv and 0.18 mSv, respectively. Figure 3 shows measured attenuation maps and ECT images in the phantom study using three different activities of external sources. Attenuation coefficients for water in TCT images and cross-calibrated SPECT values in ECT images were indicated in Table 1. Table 2 shows attenuation coefficients and SPECT values acquired with the I-T3-E3 and I-T1E2 methods. TCT images and ECT images of a normal volunteer who underwent the T3-I-E3 protocol are

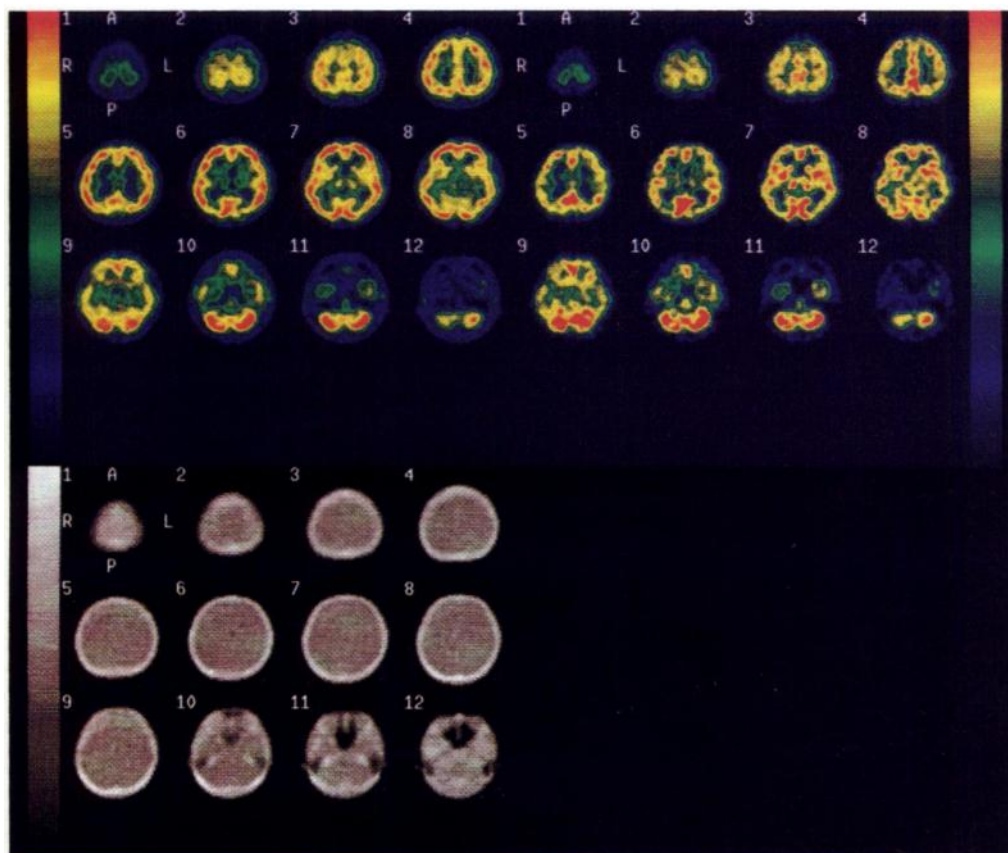


FIGURE 4. ECT images without correction (upper left), with correction (upper right) and TCT images (lower) of a normal volunteer acquired with the T3-I-E3 protocol.

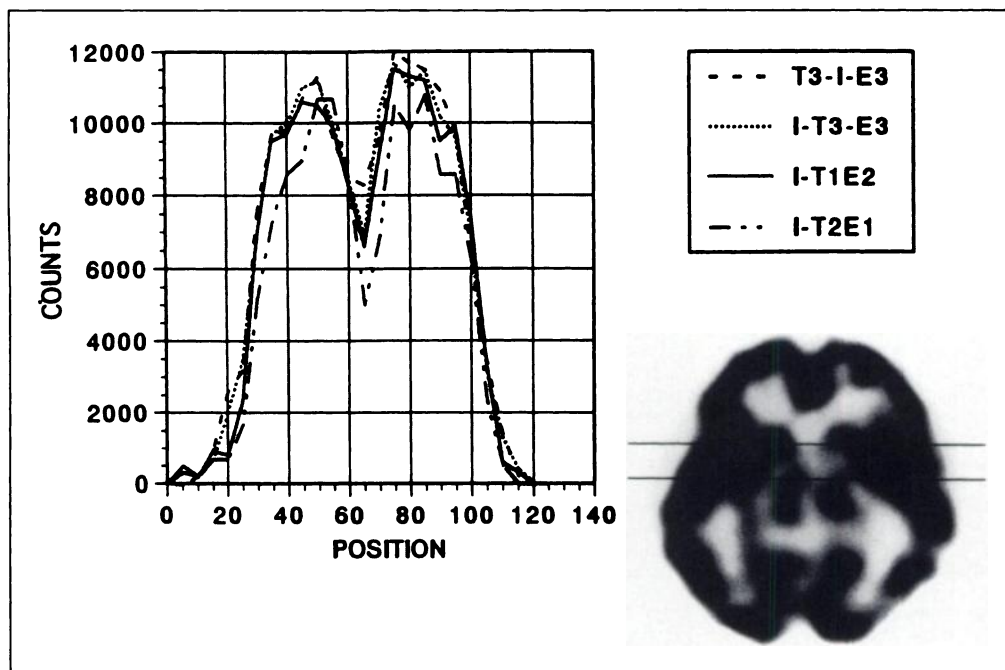


FIGURE 5. Count profile curves obtained from ECT images with scatter and attenuation correction.

shown in Figure 4. Figure 5 includes count profile curves obtained from another volunteer acquired with each of the four protocols.

DISCUSSION

For reconstruction of quantitative SPECT images, it is important to perform proper attenuation correction on the scatter-corrected data that consists of primary photons. Many methods have been proposed to compensate for the counts of scattered photons from planar images or reconstructed images (3,4,23–33). To remove scattered photons, we have to recognize that the amount of scattered photons varies pixel by pixel in a projection image depending on many factors, which include source and object distributions, object sizes and source energies. Therefore, position-dependent scatter correction, such as the TEW method, is indispensable to reconstruct quantitative SPECT images.

Radionuclide transmission CT has been reported by many investigators (10,11,13–17,21,34–36), and several gamma camera manufacturers now market radionuclide transmission scan-based attenuation correction algorithms. Sealed or unsealed radionuclides are used for the transmission source. The former is easy to prepare but expensive. On the other hand, the latter is more difficult to handle but inexpensive, especially when ^{99m}Tc is used. An additional important advantage of unsealed transmission sources for attenuation correction is their adaptability to other radionuclides, such as ^{131}I . When the injected radionuclide is the same as the transmission source, data subtraction is required after simultaneous acquisition of the emission and transmission data. The signal-to-noise ratio is lowered by the subtraction process. On the other hand, when two different radionuclides are used, the signal-to-noise ratio in the raw data is preserved, even if subtraction is performed. However, the transmission source (other than ^{99m}Tc) is more expensive. We chose ^{99m}Tc as the transmission source mainly because of its cost-effectiveness. A basic experiment using the brain phantom was obtained to consider the effect of the statistical error (37). In this study, attenuation coefficients and reconstructed SPECT values were obtained under the TCT scan time ranging from 1 to 30 min. The results showed that mean reconstructed values were

stable when the TCT data were acquired for 9 min or more and that the s.d. in the values reflecting the statistical noise was also permissible under these conditions.

There are some types of geometric relations between the transmission source and collimator (10,11,14,15,34–36). We used a combination of a line source and a fanbeam collimator (36). This combination offers some advantages, including small fractions of scattered photons, a low-dose content of the transmission source and easy handling of the source. Our collimators have a short focal length so that the detectors compose a closed triangle whose apexes are concordant with the foci of the collimators. There is no image truncation in this situation.

We used two kinds of protocols: a sequential mode and a simultaneous mode. The sequential mode requires separate transmission and emission scans that bring us only one advantage and some disadvantages. The advantage is that there is no cross-contamination between the emission and transmission projection. On the other hand, it takes more time to complete two scans, and it is probable that patient movement between the two scans will lead to misregistration of the two sets of data. In the simultaneous mode, only one scan is obtained to reduce time for acquisition and avoid misregistration. The most important characteristic of our method is that the TEW method and the fanbeam collimators work together to eliminate scattered photons emitted from the administered tracer and the external sources. Because of this correction, we could obtain scatter-corrected emission data and an accurate attenuation map even if emission and transmission scans are done simultaneously. As shown in Figure 5, the I-T1E2 method seems to be superior to the I-T2E1 method in quantification, probably due to the larger amount of primary photons detected by two gamma cameras. Additional materials required for this method are an acrylic rod, which costs less than \$100, and 222 MBq ^{99m}Tc obtained by milking. Collimators are the same as those used in conventional imaging. Additional scanning time was 15 min.

In view of all these factors, I-T1-E2 method seems to be a most promising protocol for obtaining quantitative SPECT images in clinical practice.

ACKNOWLEDGMENTS

We thank T. Sammiya, R. Iwasaki and M. Matsuda for their assistance in performing basic experiments. This work was supported in part by the Department of Education of Japan, grant 07457202 in aid for scientific research.

REFERENCES

- Ogawa K, Harata Y, Ichihara T, et al. Estimation of scatter component in SPECT planar image using a Monte Carlo simulation. *Kaku Igaku* 1990;27:467-475.
- Floyd CE, Jaszczak RJ, Harris CC, et al. Energy and spatial distribution of multiple order Compton scatter in SPECT: a Monte Carlo simulation. *Phys Med Biol* 1984;29:1217-1230.
- Ogawa K, Harata Y, Ichihara T, et al. A practical method for position-dependent Compton-scatter correction in single-photon emission CT. *IEEE Trans Med Imag* 1991;10:408-412.
- Ichihara T, Ogawa K, Motomura N, et al. Compton scatter correction using triple-energy window method for single- and dual-isotope SPECT. *J Nucl Med* 1993;34:2216-2221.
- Ogawa K, Ichihara T, Kubo A. Accurate scatter correction in single-photon emission CT. *Ann Nucl Med Sci* 1994;7:145-150.
- Sorenson JA. Quantitative measurement of radioactivity in vivo by whole-body counting. In: *Instrumentation in nuclear medicine*, vol. 2. New York, NY; Academic Press: 1974:311-348.
- Chang LT. A method for attenuation correction in radionuclide computed tomography. *IEEE Trans Nucl Sci* 1978;25:638-642.
- Bellini S, Piacentini M, Caffolio C, Rocca F. Compensation of tissue absorption in emission tomography. *IEEE Trans Acoustics, Speech, Signal Process* 1979;27:213-218.
- Tanaka E, Toyama H, Murayama H. Convolutional image registration for quantitative SPECT. *Phys Med Biol* 1984;29:1489-1500.
- Ogawa K, Takagi Y, Kubo A, et al. An attenuation correction method of SPECT using gamma ray transmission CT. *Jpn J Nucl Med* 1985;22:477-490.
- Bailey DL, Hutton BF, Walker PJ. Improved SPECT using simultaneous emission and transmission tomography. *J Nucl Med* 1987;28:844-851.
- Manglos SH, Jaszczak RJ, Floyd CE, et al. Nonisotropic attenuation in SPECT: phantom tests in quantitative effects and compensation techniques. *J Nucl Med* 1987;28:1584-1591.
- Ljunberg M, Strand SV. Attenuation correction in SPECT-based on transmission studies and Monte Carlo simulations of build-up functions. *J Nucl Med* 1990;31:493-500.
- Manglos SH, Bassano DA, Duxbury CE, Capone RB. Attenuation maps for SPECT determined using cone-beam transmission computed tomography. *IEEE Trans Nucl Sci* 1990;31:600-608.
- Manglos SH, Capone RB, Bassano DA. Detection of nonuniformity measurements and corrections for cone beam transmission CT on a gamma camera. *Am Assoc Phys Med* 1992;19:491-500.
- Lang TF, Hasegawa BH, Liew SC, et al. Description of a prototype emission transmission computed tomography imaging system. *J Nucl Med* 1992;33:1881-1887.
- Gullberg GT, Zeng GL, Datz FL, et al. Review of convergent beam tomography in SPECT. *Phys Med Biol* 1992;37:507-534.
- Kemp BJ, Prato FS, Dean GW, Nicholson RL, Resse L. Correction for attenuation in ^{99m}Tc -HMPAO SPECT brain imaging. *J Nucl Med* 1992;33:1875-1880.
- Galt JR, Cullom SJ, Garcia EV. SPECT quantification: a simplified method of attenuation and scatter correction for cardiac imaging. *J Nucl Med* 1992;33:2232-2237.
- Pan X, Wong WH, Chen C, Lin J. Correction for photon attenuation in SPECT: analytical framework; average factors, and a new hybrid approach. *Phys Med Biol* 1993;38:1219-1234.
- Frey EC, Tsui BMW, Perry JR. Simultaneous acquisition of emission and transmission data for improved ^{201}Tl cardiac SPECT imaging using a ^{99m}Tc transmission source. *J Nucl Med* 1992;33:2238-2245.
- Ichihara T, Motomura N, Hasegawa H, et al. Simultaneous emission transmission scan for the measurement of three-dimensional absolute activity distribution using dual isotope, TEW scatter compensation method and fanbeam collimation. *Conf Rec IEEE Nucl Sci Sym* 1995:1275-1279.
- Axelsson B, Msaki B, Israelsson A. Subtraction of Compton-scattered photons in SPECT. *J Nucl Med* 1984;25:490-494.
- Floyd CE, Jaszczak RJ, Greer KL, Coleman RE. Deconvolution of Compton scatter in SPECT. *J Nucl Med* 1985;26:403-408.
- Msaki B, Axelsson B, Larsson SA. Some physical factors influencing the accuracy of convolution scatter correction in SPECT. *Phys Med Biol* 1988;34:283-298.
- Jaszczak RJ, Greer KL, Floyd CE, Harris CC, Coleman RE. Improved SPECT quantification using compensation for scattered photons. *J Nucl Med* 1984;25:893-900.
- Koral KF, Swailem FM, Buchbinder S, et al. SPECT dual-energy window Compton correction: scatter multiplier required for quantification. *J Nucl Med* 1990;31:90-98.
- Hamill JJ, DeVitro RP. Scatter reduction with energy-weighted acquisition. *IEEE Trans Nucl Sci* 1989;36:1334-1339.
- Halama JR, Henkin RE, Friend LE. Gamma camera radionuclide images: improved contact with energy-weighted acquisition. *Radiology* 1988;169:533-538.
- Koral KF, Wang X, Rogers WL, et al. SPECT Compton-scatter correction by analysis of energy spectra. *J Nucl Med* 1988;29:195-202.
- Gagnon D, Todd-Pokropek AE, Arsenault A, Dupras G. Introduction to holospectral imaging in nuclear medicine for scatter subtraction. *IEEE Trans Med Imaging* 1989;8:245-250.
- Floyd CE, Jaszczak RJ, Greer KL, Coleman RE. Inverse Monte Carlo as a unified reconstruction algorithm for ECT. *J Nucl Med* 1986;27:1577-1585.
- Koral KF, Cinthorne NH, Rogers WL. Improving emission-computed tomography quantification by Compton-scatter rejection through offset window. *Nuclear Instrum Methods Phys Res* 1986;A242:610-614.
- Manglos SH. Truncation artifact suppression in cone-beam radionuclide transmission CT using maximum likelihood techniques: evaluation with human subjects. *Phys Med Biol* 1992;37:549-562.
- Tan P, Bailey DL, Meikle SR, et al. A scanning line source for simultaneous emission and transmission measurements in SPECT. *J Nucl Med* 1993;34:1752-1760.
- Jaszczak RJ, Gilland DR, Hanson HW, et al. Fast transmission CT for determining attenuation maps using a collimated line source, rotatable air-copper-lead attenuators and fanbeam collimation. *J Nucl Med* 1993;34:1577-1586.
- Hasegawa H, Motomura N, Ichihara T, Ogawa K, Kubo A. Evaluation of SPECT quantification using transmission computed tomography [Abstract]. *Jpn J Nucl Med* 1995;32:776P.